Self-energy renormalization around the flux phase in the *t-J* model: Possible implications in underdoped cuprates

Andrés Greco
Facultad de Ciencias Exactas, Ingeniería y Agrimensura and Instituto de Física Rosario (UNR-CONICET), Avenida Pellegrini, 250-2000 Rosario, Argentina

(Received 11 December 2007; revised manuscript received 4 February 2008; published 6 March 2008)

The flux phase predicted by the *t-J* model in the large-*N* limit exhibits features that make it a candidate for describing the pseudogap regime of cuprates. However, certain properties, such as, for instance, the prediction of well-defined quasiparticle peaks, speak against this scenario. We have addressed these issues by computing self-energy renormalizations in the vicinity of flux phase. The calculated spectral functions show features similar to those observed in experiments. At low doping, near the flux phase, the spectral functions are anisotropic on the Fermi surface and very incoherent near the hot spots. The temperature and doping evolution of self-energy and spectral functions are discussed and compared with the experiment.

DOI: 10.1103/PhysRevB.77.092503 PACS number(s): 74.72.−h, 71.10.Fd, 71.27.+a

The pseudogap (PG) phase of high-T_c cuprates presents unusual properties in clear contrast to those expected for conventional metals[1] and, in spite of the many scenarios proposed, the problem remains open. A well-known phenomenological theory is the *d*-CDW (where CDW denotes charge-density wave),[2] in which a normal state (NS) gap was proposed. Interestingly, *d*-CDW is closely related to the flux phase (FP), which was formerly predicted in the context of the *t-J* model.[3] In both scenarios, the PG coexists and competes with superconductivity, is complex, and shows *d*-wave symmetry. FP was also studied by means of different analytical and numerical methods.[4–7] In the mean-field approximation of the *t-J* model, below a characteristic temperature T^*, a *d*-wave NS gap opens on the Fermi surface (FS) near the hot spots $[\mathbf{k}\cong(0,\pi)]$. This leads to pockets with low spectral weight intensity in the outer section.[8] Thus, these pockets resemble the arcs observed in angle-resolved photoelectron spectroscopy (ARPES) experiments.[9] Furthermore, recent progress on the *t-J* model shows that the competition between FP and superconductivity leads to a phase diagram qualitatively similar to that observed in cuprates.[5] Raman and tunneling spectroscopy results show similarities with the experiment.[10] Very recent ARPES,[11] Raman,[12] specific heat,[13] and femtosecond optical pulse[14] experiments together with some theoretical developments[15] support the competing two-gap scenario. From the above reasons, FP may be considered as a good candidate for describing the PG region. Nevertheless, there are some drawbacks to be addressed. While in the FP scenario a true phase transition occurs at T^*, many experiments show a smooth behavior as a function of temperature.[16] In addition, well-defined quasiparticle (QP) peaks are predicted everywhere on the Brillouin zone, above and below T^*, while experiments show that the QP exists only near the nodal direction.[17] Near hot spots, coherent peaks are observed neither below nor above the PG temperature in apparent contradiction with the FP picture. On the other hand, the PG observed in ARPES, consistent with tunneling experiments,[18] seems to be filling up but is not closing,[19] leading to a smooth evolution of spectral properties.

In spite of the above objections, we will assume the point of view that the basic physics of cuprates is contained in the *t-J* model (see Ref. 20 for discussions). Moreover, to address the above discussion, it is necessary to perform a controllable self-energy and spectral function calculation beyond mean field. Recently, a large-*N* approach for the *t-J* model based on the path integral representation for *X* operators was proposed.[6] At the mean-field level, the approach of Ref. 6 agrees with slave boson[3,4] and the approach of Ref. 5. Additionally, it can be easily applied beyond mean field, allowing the calculation of self-energy and spectral functions.[21] In this Brief Report, we discuss spectral functions and self-energy calculations in the NS in the vicinity to the FP instability. We have found that the spectral functions and the corresponding self-energies are very anisotropic on the FS, leading to a well-defined QP near the nodal direction and very incoherent features near the hot spots.

We study the two-dimensional *t-J* model with hopping *t* and Heisenberg coupling $J/t=0.3$ between nearest-neighbor sites on the square lattice.[22] In the following, energy is in units of *t*. Using the formulation described in Ref. 6, the mean-field homogeneous Fermi liquid (HFL) becomes unstable when the static ($\omega=0$) flux susceptibility $\chi_{flux}(\mathbf{q},\omega)=\left(\frac{\delta}{2}\right)^2[(8/J)\Delta^2-\Pi(\mathbf{q},\omega)]^{-1}$ diverges. $\Pi(\mathbf{q},\omega)$ is an electronic bubble calculated with a form factor $\gamma(\mathbf{q},\mathbf{k})=2\Delta[\sin(k_x-q_x/2)-\sin(k_y-q_y/2)]$.[6,21,23] (For the definition of Δ, see below.) In Fig. 1(a), the phase diagram in the doping-temperature (δ-T) plane is presented, where T^* indicates the FP instability onset. At $T=0$, a phase transition occurs at the critical doping $\delta_c\cong 0.12$ for the incommensurate critical vector $\mathbf{q}_c\cong(1,0.86)\pi$ near (π,π). At finite T, the instability is commensurate $[\mathbf{q}_c=(\pi,\pi)]$. Therefore, since the instability takes place at, or close to, (π,π), the form factor $\gamma(\mathbf{q},\mathbf{k})$ transforms to $\sim[\cos(k_x)-\cos(k_y)]$, which indicates the *d*-wave character of the FP. Since T^* falls abruptly to zero at δ_c,[24] we associate the FP with the scenario discussed in Fig. 1(a) of Ref. 16. In Fig. 1(b), we have plotted $\mathrm{Im}\,\chi_{flux}(\mathbf{q}=(\pi,\pi),\omega)$ at $T=0$, which shows that when $\delta\to\delta_c$, a low-energy *d*-wave flux mode becomes soft, accumulating large spectral weight. This soft mode reaches $\omega=0$ at $\delta=\delta_c$, freezing the FP.

For studying the soft mode influence on one-electron

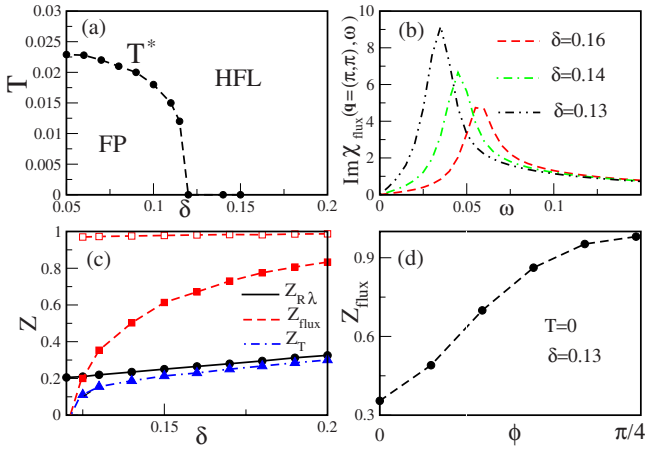

FIG. 1. (Color online) (a) Large-N t-J model phase diagram in the δ-T plane. (b) Softening of the d-wave flux mode for several δ values approaching $\delta_c \cong 0.12$. (c) QP weight Z for $\Sigma_{R\lambda}$ (black circles), Σ_{flux} (red squares), and Σ_T (blue triangles). (d) Z_{flux} versus the FS angle ϕ for $\delta=0.13$.

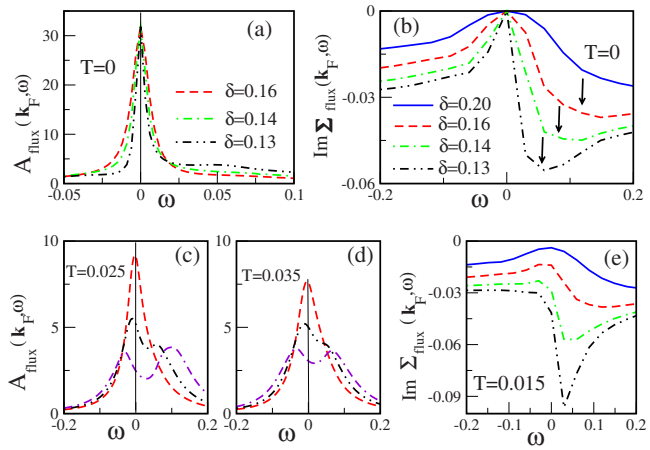

FIG. 2. (Color online) (a) $T=0$ spectral functions at the antinodal k_F for several doping values approaching δ_c. A broadening $\eta=0.01$ was used in the calculation. The vertical line marks the Fermi level. (b) $T=0$ flux scattering rate for several δ values at the antinodal k_F. [(c) and (d)] Spectral functions at the antinodal k_F for $T=0.025$ and $T=0.035$, respectively, for $\delta=0.16$ (red dashed line), $\delta=0.13$ (black double-dotted-dashed line), and $\delta=0.10$ (violet double-dashed-dotted line). (e) The same as in (b), but for $T=0.015$.

spectral properties, we calculate self-energy renormalizations in the NS in the vicinity of T^*. The inclusion of the superconducting ground state in the calculation does not change significantly the FP region (see Refs. 5 and 10). After collecting all contributions in $\mathcal{O}(1/N)$, the self-energy can be written as[21] [in $\mathcal{O}(1/N)$, the inclusion of self-energy corrections in the calculation of electronic bubbles is not necessary]

$$\mathrm{Im}\,\Sigma_T(\mathbf{k},\omega) = \mathrm{Im}\,\Sigma_{R\lambda}(\mathbf{k},\omega) + \mathrm{Im}\,\Sigma_{flux}(\mathbf{k},\omega), \tag{1}$$

where

$$\begin{aligned}\mathrm{Im}\,\Sigma_{R\lambda}(\mathbf{k},\omega) = -\frac{1}{N_s}\sum_{\mathbf{q}} \{&\Omega^2\,\mathrm{Im}[D_{RR}(\mathbf{q},\omega-\epsilon_{k-q})] \\ &+ 2\Omega\,\mathrm{Im}[D_{\lambda R}(\mathbf{q},\omega-\epsilon_{k-q})] \\ &+ \mathrm{Im}[D_{\lambda\lambda}(\mathbf{q},\omega-\epsilon_{k-q})]\} \\ &\times[n_F(-\epsilon_{k-q}) + n_B(\omega-\epsilon_{k-q})]\end{aligned} \tag{2}$$

and

$$\begin{aligned}\mathrm{Im}\,\Sigma_{flux}(\mathbf{k},\omega) = -\frac{1}{N_s}\sum_{\mathbf{q}} &\gamma^2(\mathbf{q},\mathbf{k})\mathrm{Im}\,\chi_{flux}(\mathbf{q},\omega-\epsilon_{k-q}) \\ &\times[n_F(-\epsilon_{k-q}) + n_B(\omega-\epsilon_{k-q})].\end{aligned} \tag{3}$$

In the above expressions, $\Omega=(\varepsilon_{k-q}+\omega+\mu)/2$, $\varepsilon_k = (t\delta+\Delta)[\cos(k_x)+\cos(k_y)]$ is the mean-field electronic dispersion, $\epsilon_k=\varepsilon_k-\mu$, and $\Delta=\frac{J}{2N_s}\Sigma_k \cos(k_x)n_F(\epsilon_k)$. n_B (n_F) is the Bose (Fermi) factor, μ is the chemical potential, and N_s is the number of sites. $\Sigma_{R\lambda}$ corresponds to the charge (δR) sector, nondouble occupancy ($\delta\lambda$) sector, and the mixing of both.[21,25] Since for $J=0.3$ there is no important influence of J contributions in $\Sigma_{R\lambda}$, then $\Sigma_{R\lambda}$ is close to the self-energy for $J=0$. Instead, Σ_{flux} is dominated by J. The explicit expressions of D_{RR}, $D_{\lambda R}$, and $D_{\lambda\lambda}$ are given in Ref. 21.

In Fig. 1(c), we have plotted the QP weight $Z=1/(1-\partial\,\mathrm{Re}\,\Sigma/\partial\omega)$ vs δ for each self-energy contribution. $Z_{R\lambda}$ (black circles) are results at the Fermi crossing momentum in the $(0,0)$-$(0,\pi)$ direction (antinodal k_F). $Z_{R\lambda}$ decreases (linearly) with decreasing doping ($Z_{R\lambda}\to 0$ when $\delta\to 0$). Due to the fact that $\Sigma_{R\lambda}$ is very isotropic on the FS, results for $Z_{R\lambda}$ at the Fermi crossing momentum in the nodal direction (nodal k_F) are very similar to those for the antinodal k_F. In contrast, Z_{flux} (red squares) is strongly anisotropic on the FS. For nodal k_F (open red squares), $Z_{flux}\sim 1$, which means that Σ_{flux} has no important contribution near the nodal direction. For antinodal k_F (closed red squares), Z_{flux} is rapidly decreasing with doping, i.e., $Z_{flux}\to 0$ when $\delta\to\delta_c$, where the flux instability takes place. In order to show explicitly the anisotropy of Σ_{flux}, in Fig. 1(d), we have plotted Z_{flux} versus the FS angle ϕ from $\phi=0$ (antinodal k_F) to $\phi=\pi/4$ (nodal k_F) for $\delta=0.13$. The soft d-wave mode [Fig. 1(b)], which scatters electrons on the FS with momentum transfer $\mathbf{q}\sim(\pi,\pi)$, is responsible for the observed anisotropy. By using $Z_{R\lambda}$ and Z_{flux}, the total QP weight can be written as $Z_T=1/(Z_{R\lambda}^{-1}+Z_{flux}^{-1}-1)$. Blue triangles are the results for Z_T at the antinodal k_F. While for large δ, self-energy renormalizations are dominated by $\Sigma_{R\lambda}$, Σ_{flux} dominates near δ_c. Results for Z_T at the nodal k_F (not shown) follow the same trend as $Z_{R\lambda}$, i.e., the nodal Z_T exhibits a linear behavior with slope similar to that discussed in Ref. 26.

Next we will consider the Σ_{flux} contribution to the spectral function $A_{flux}(\mathbf{k},\omega)$. Spectral functions for different δ values near δ_c at the antinodal k_F are presented for $T=0$ in Fig. 2(a). When $\delta\to\delta_c$, the area under the QP peak decreases (consistent with the behavior of Z_{flux}) and spectral weight is transferred to the incoherent structure at about $\omega\sim 0.05-0.1t$. Figure 2(b) shows the ω behavior of the flux scattering rate $\mathrm{Im}\,\Sigma_{flux}$ at the antinodal k_F for several δ values near δ_c. With

decreasing doping toward δ_c, Im Σ_{flux} evolves from a Fermi-liquid (FL)-like behavior ($\sim\omega^2$) (see solid line for δ=0.20) to a non-FL-like behavior ($\sim\omega$) (see double-dotted-dashed line for δ=0.13). At the same time, the structures (marked with arrows) that appear at low energy are correlated with the soft mode discussed in Fig. 1(b). Im Σ_{flux} at the nodal k_F (not shown) is weaker than for the antinodal k_F and, in addition, it shows a FL-like behavior for all δ values. In summary, as observed in experiments,[27,28] at low doping the scattering rate is strongly anisotropic on the FS, presenting a FL-like ($\sim\omega^2$) behavior near the nodal k_F and a non-FL-like ($\sim\omega$) behavior near the antinodal k_F. In addition, this anisotropy disappears with overdoping, where the behavior is more FL-like.

In Figs. 2(c) and 2(d), spectral functions at the antinodal k_F are presented for T=0.025 and T=0.035, respectively. For a given temperature, the intensity at the FS increases with increasing doping, showing, consistent with experiments,[17,27] a more clearly defined QP peak with overdoping. The following behavior is also interesting. For instance, for T=0.035, with decreasing doping while the peak at the Fermi level loses intensity, a broad shoulder appears at positive ω together with an apparent gaplike (which is not a true gap) structure. As suggested by ARPES experiments,[9,19] with increasing temperature, the gaplike features seem to be filling up but are not closing (see results for δ=0.10). Notice that for δ=0.10, the leading edge below the FS is at $\omega=-0.05t$ which, using t=0.4 eV, is about 20–30 meV, thus, of the order of the observed PG value.[19] Therefore, spectral functions are strongly temperature dependent, even at temperatures much lower than the hopping t, showing broad features at the antinodal k_F. Spectral functions are nearly doping and temperature independent at the nodal k_F and show well-defined QP peaks as in experiments.[17,27] As mentioned above, at the mean-field level, when the temperature decreases, a gap opens at T^* near the hot spots. However, beyond mean field, spectral functions are very incoherent above T^*, showing that features expected to occur for $T<T^*$ already appear for $T>T^*$ due to self-energy renormalizations. For instance, the coherence loss when going from nodal k_F to antinodal k_F may suggest the appearance of arcs. Therefore, we think that self-energy corrections could be masking a likely abrupt change at T^* given the appearance, in agreement with observations, of a smooth crossover. In addition, it may probably be that T^* determined from the ARPES line shape is somewhat shifted from the temperature at which PG opens.

The above results are due to the doping and temperature behavior of the self-energy. In Fig. 2(e), we present results for Im Σ_{flux} at T=0.015 for several δ values at the antinodal k_F. While for δ=0.20 Im Σ_{flux} shows, as expected for a FL, the maximum at the Fermi level, with decreasing doping (see, for instance, double-dotted-dashed line for δ=0.13) the maximum is shifted with respect to ω=0. As discussed in Refs. 29 and 30, this behavior can damage the quasiparticle FL picture. For nodal k_F, the situation is FL-like, e.g., Im Σ_{flux} shows, for all doping values, the maximum at ω=0, which increases with T as $\sim T^2$. Notice the similarities between our self-energy results in Fig. 2(e) and those discussed in Ref. 30.

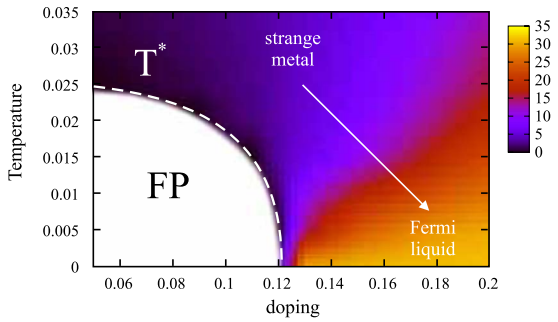

FIG. 3. (Color online) ω=0 spectral function intensity at the antinodal k_F in the δ-T plane.

In Fig. 3, the ω=0 spectral function intensity at the antinodal k_F is presented in the δ-T plane. The spectral intensity distribution suggests a crossover from a strange metal at low doping and high temperature to a FL at high doping and low temperature. Based on different arguments, recent works have proposed a similar picture.[31]

Before closing, let us discuss the influence of $\Sigma_{R\lambda}$ on previous results. In Fig. 4(a), self-energy results for $\Sigma_{R\lambda}$, Σ_{flux}, and Σ_T, at the antinodal k_F, are presented for δ=0.13 and T=0.02. Im $\Sigma_{R\lambda}$ (solid line) shows a FL-like behavior near ω=0. The dotted-dashed line is the result for Im Σ_T [Eq. (1)]. While at large frequency Σ_T is dominated by $\Sigma_{R\lambda}$, properties near the FS are dominated by Σ_{flux}. Im Σ_T at the nodal k_F is very similar to Im $\Sigma_{R\lambda}$ (solid line) because Σ_{flux} has no important influence on the nodal direction. In Fig. 4(b), using Σ_T, the total spectral functions at the nodal k_F (solid line) and at the antinodal k_F (dashed line) are presented for low ω. For the spectral function behavior at large ω, see Ref. 21. Although $\Sigma_{R\lambda}$ might modify our previous results, it remains the main tendency arising from Σ_{flux}, i.e., the spectral functions are strongly anisotropic on the FS, losing intensity and becoming broad when going from nodal k_F to antinodal k_F.

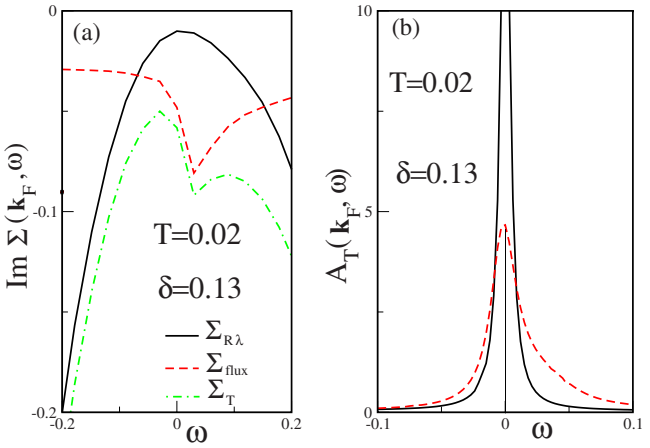

FIG. 4. (Color online) (a) Scattering rate at the antinodal k_F for δ=0.13 and T=0.02 for Σ_{flux} (dashed line), $\Sigma_{R\lambda}$ (solid line), and Σ_T (dotted-dashed line). (b) Total spectral function (calculated using Σ_T) for δ=0.13 and T=0.02 at the nodal k_F (solid line) and antinodal k_F (dashed line). The intensity at the nodal k_F was cut for clarity reasons.

Concluding, in the framework of the t-J model, we have computed self-energy corrections in the vicinity of the FP instability. The corresponding spectral functions are anisotropic on the FS and very incoherent near hot spots, thus they show features similar to those observed in experiments. In agreement with recent discussions (see Ref. 28 and references therein), our results show two contributions to the scattering channel. One contribution (Σ_{flux}) is strongly anisotropic on the FS; the other one ($\Sigma_{R\lambda}$) is very isotropic. Σ_{flux} dominates at low doping (near δ_c) and low energy, being relevant for the PG properties. In contrast, $\Sigma_{R\lambda}$ dominates at large doping and large ω. In Ref. 32, by means of transport measurements, it was found that an isotropic scattering channel dominates in overdoped samples, which agrees with our predictions for $\Sigma_{R\lambda}$. In a recent work,[33] it was proposed that the high-energy features observed in ARPES[34] may be due to the large ω behavior of $\Sigma_{R\lambda}$. Finally, our results indicate that some problems, which can be interpreted against the FP scenario, may be less serious after including self-energy renormalizations.

The author thanks M. Bejas, A. Foussats, H. Parent, A. Muramatsu, and R. Zeyher for valuable discussions.

[1] T. Timusk and B. Statt, Rep. Prog. Phys. **62**, 61 (1999).
[2] S. Chakravarty, R. B. Laughlin, D. K. Morr, and C. Nayak, Phys. Rev. B **63**, 094503 (2001).
[3] I. Affleck and J. B. Marston, Phys. Rev. B **37**, 3774 (1988); T. C. Hsu, B. J. Marston, and I. Affleck, *ibid.* **43**, 2866 (1991).
[4] D. C. Morse and T. C. Lubensky, Phys. Rev. B **42**, 7994 (1990).
[5] E. Cappelluti and R. Zeyher, Phys. Rev. B **59**, 6475 (1999).
[6] A. Foussats and A. Greco, Phys. Rev. B **70**, 205123 (2004).
[7] P. W. Leung, Phys. Rev. B **62**, R6112 (2000).
[8] S. Chakravarty, C. Nayak, and S. Tewari, Phys. Rev. B **68**, 100504(R) (2003).
[9] M. R. Norman, H. Ding, M. Randeria, J. C. Campuzano, T. Yokoya, T. Takeuchi, T. Takahashi, T. Mochiku, K. Kadowaki, P. Guptasarma, and D. G. Hinks, Nature (London) **392**, 157 (1998).
[10] R. Zeyher and A. Greco, Phys. Rev. Lett. **89**, 177004 (2002); A. Greco and R. Zeyher, Phys. Rev. B **70**, 024518 (2004).
[11] T. Kondo, Tsunehiro Takeuchi, Adam Kaminski, Syunsuke Tsuda, and Shik Shin, Phys. Rev. Lett. **98**, 267004 (2007); M. Hashimoto, T. Yoshida, K. Tanaka, A. Fujimori, M. Okusawa, S. Wakimoto, K. Yamada, T. Kakeshita, H. Eisaki, and S. Uchida, Phys. Rev. B **75**, 140503(R) (2007).
[12] M. Le Tacon, A. Sacuto, Y. Gallais, D. Colson, and A. Forget, Phys. Rev. B **76**, 144505 (2007).
[13] H.-H. Wen and X.-G. Wen, Physica C **460**, 28 (2007).
[14] E. E. M. Chia, J.-X. Zhu, D. Talbayev, R. D. Averitt, A. J. Taylor, K. H. Oh, I. S. Jo, and S. I. Lee, Phys. Rev. Lett. **99**, 147008 (2007).
[15] B. Valenzuela and E. Bascones, Phys. Rev. Lett. **98**, 227002 (2007); T. Das, R. S. Markiewicz, and A. Bansil, arXiv:0711.0480 (unpublished).
[16] J. L. Tallon and J. W. Loran, Physica C **349**, 53 (2001).
[17] C. Kim, P. J. White, Z.-X. Shen, T. Tohyama, Y. Shibata, S. Maekawa, B. O. Wells, Y. J. Kim, R. J. Birgeneau, and M. A. Kastner, Phys. Rev. Lett. **80**, 4245 (1998).
[18] C. Renner, B. Revaz, J. Y. Genoud, K. Kadowaki, and Ø. Fischer, Phys. Rev. Lett. **80**, 149 (1998).
[19] M. R. Norman, M. Randeria, H. Ding, and J. C. Campuzano, Phys. Rev. B **57**, R11093 (1998).
[20] P. Lee, N. Nagaosa, and X.-G. Wen, Rev. Mod. Phys. **78**, 17 (2006).
[21] M. Bejas, A. Greco, and A. Foussats, Phys. Rev. B **73**, 245104 (2006).
[22] For simplicity and without losing generality, we have considered the minimal t-J model. The inclusion of hopping between second, third, etc., neighbor sites produces only small quantitative but not qualitative changes.
[23] This form factor is obtained after projecting the electron-boson vertex [Eq. (9) of Ref. 6] on the corresponding eigenvector for the FP instability.
[24] The inclusion of a hopping between second neighbors $t'/t=0.35$ simply shifts δ_c to values closer to the experimental (Ref. 16) $\delta_c \sim 0.19$ (see Ref. 10).
[25] δR is the fluctuation of the charge Hubbard operator X^{00} [$X^{00}=\delta(1+\delta R)$] associated with the number of holes. $\delta\lambda$ is the fluctuation of the Lagrangian multiplier related to the non-double-occupancy constraint $X^{00}+\Sigma_\sigma X^{\sigma\sigma}=1$.
[26] T. Yoshida, X. J. Zhou, T. Sasagawa, W. L. Yang, P. V. Bogdanov, A. Lanzara, Z. Hussain, T. Mizokawa, A. Fujimori, H. Eisaki, Z.-X. Shen, T. Kakeshita, and S. Uchida, Phys. Rev. Lett. **91**, 027001 (2003).
[27] A. Kaminski, H. M. Fretwell, M. R. Norman, M. Randeria, S. Rosenkranz, U. Chatterjee, J. C. Campuzano, J. Mesot, T. Sato, T. Takahashi, T. Terashima, M. Takano, K. Kadowaki, Z. Z. Li, and H. Raffy, Phys. Rev. B **71**, 014517 (2005).
[28] J. Chang, M. Shi, S. Pailhes, M. Maansson, T. Claesson, O. Tjernberg, A. Bendounan, L. Patthey, N. Momono, M. Oda, M. Ido, C. Mudry, and J. Mesot, arXiv:0708.2782 (unpublished).
[29] A. A. Katanin and A. P. Kampf, Phys. Rev. Lett. **93**, 106406 (2004).
[30] L. Dell'Anna and W. Metzner, Phys. Rev. B **73**, 045127 (2006).
[31] H. Castro and G. Deutscher, Phys. Rev. B **70**, 174511 (2004); A. Kaminski, S. Rosenkranz, H. M. Fretwell, Z. Z. Li, H. Raffy, M. Randeria, M. R. Norman, and J. C. Campuzano, Phys. Rev. Lett. **90**, 207003 (2003).
[32] S. Nakamae, K. Behnia, N. Mangkorntong, M. Nohara, H. Takagi, S. J. C. Yates, and N. E. Hussey, Phys. Rev. B **68**, 100502(R) (2003).
[33] A. Greco, Solid State Commun. **142**, 318 (2007).
[34] B. Xie, K. Yang, D. W. Shen, J. F. Zhao, H. W. Ou, J. Wei, S. Y. Gu, M. Arita, S. Qiao, H. Namatame, M. Taniguchi, N. Kaneko, H. Eisaki, K. D. Tsuei, C. M. Cheng, I. Vobornik, J. Fujii, G. Rossi, Z. Q. Yang, and D. L. Feng, Phys. Rev. Lett. **98**, 147001 (2007); Z.-H. Pan, P. Richard, A. V. Fedorov, T. Kondo, T. Takeuchi, S. L. Li, Pengcheng Dai, G. D. Gu, W. Ku, Z. Wang, and H. Ding, arXiv:cond-mat/0610442.